MATRIX CRACKING IN A FIBER-REINFORCED COMPOSITE WITH SLIP AT THE FIBER–MATRIX INTERFACE

A. C. WIJEYEWICKREMA and L. M. KEER

Department of Civil Engineering, Northwestern University, Evanston, IL 60201, U.S.A.

Abstract—A linear elastic analysis is presented of interfacial slip under longitudinal tensile loading in a fiber-reinforced brittle matrix composite with matrix cracks terminating and blunting at the interface. A prescribed shear stress distribution is taken in the slip region. The interfacial adhesive shear stress in the slip region which is later assumed constant is determined for different ratios of shear moduli, fiber volume fractions and slip lengths. Stress fields are obtained for a brittle matrix fiber-reinforced composite, calcium aluminosilicate glass ceramic reinforced with silicon carbide fibers (SiC/CAS), and are compared with the case when there is perfect adhesion at the interface.

INTRODUCTION

A prime concern in the design and development of fiber-reinforced brittle matrix composites is the toughness enhancement under tensile loading due to debonding and sliding at the fiber–matrix interface. A matrix crack propagating in a plane normal to the loading direction surrounds and leaves behind the uncracked high strength fibers that bridge the crack and thereby provide resistance to the opening of the crack. This failure mechanism which results in intact fibers in the crack wake occurs when the fiber–matrix interface is relatively weak such that debonding and sliding is allowed. The main objective of this analysis is to investigate the effects of fiber volume ratio and slip length on the interfacial adhesive stress and the stress fields in the brittle matrix.

Although various models have been proposed with different simplifying assumptions by Marshall *et al.* (1985), Budiansky *et al.* (1986), Gao *et al.* (1988), McCartney (1989), Sigl and Evans (1989), Daniel *et al.* (1989) and Tsai and Mura (1991) an elasticity approach which allows for slip at the interface has not yet been presented.

The planar problem of interfacial slip due to the opening of a pressurized crack which is normal to the interface was analysed by Keer and Chen (1981) while Dollar and Steif (1989) considered a tension crack which opens at a frictional interface. Work which considers the effects of debonding and sliding in brittle matrix composites is due to Hutchinson and Jensen (1990) where debonding was treated as mode II interface fracture. Recently matrix fracture and crack interaction were studied by Wijeyewickrema and Keer (1991, 1992) but only perfectly bonded interfaces were considered. In general the interfacial shear stress in the slip zone is modeled either by the Coulomb friction law or as a prescribed variation in the slip zone. In the present study the interfacial shear stress in the slip zone is specified as constant.

FORMULATION OF THE PROBLEM

To analyse the case of interfacial slip in a fiber-reinforced brittle matrix composite under longitudinal tensile loading, shown schematically in Fig. 1(a), the axisymmetric concentric cylinders model shown in Fig. 1(b) is used. Reasons for using this axisymmetric model to approximate a hexagonal array of fibers in a matrix and references to others who have used this model are given in Wijeyewickrema and Keer (1991). Here an infinitely long elastic fiber of radius a is surrounded by an elastic matrix which has an outer radius $b = a/V_f^{1/2}$ where V_f is the fiber volume ratio of the uniaxial fiber-reinforced composite. A uniform longitudinal tensile strain ε_0 is applied to the system at $z = \pm\infty$. The crack plane which is normal to the z-axis is taken as the $z = 0$ plane and interfacial slip takes place in the region $|z| < L, r = a$.
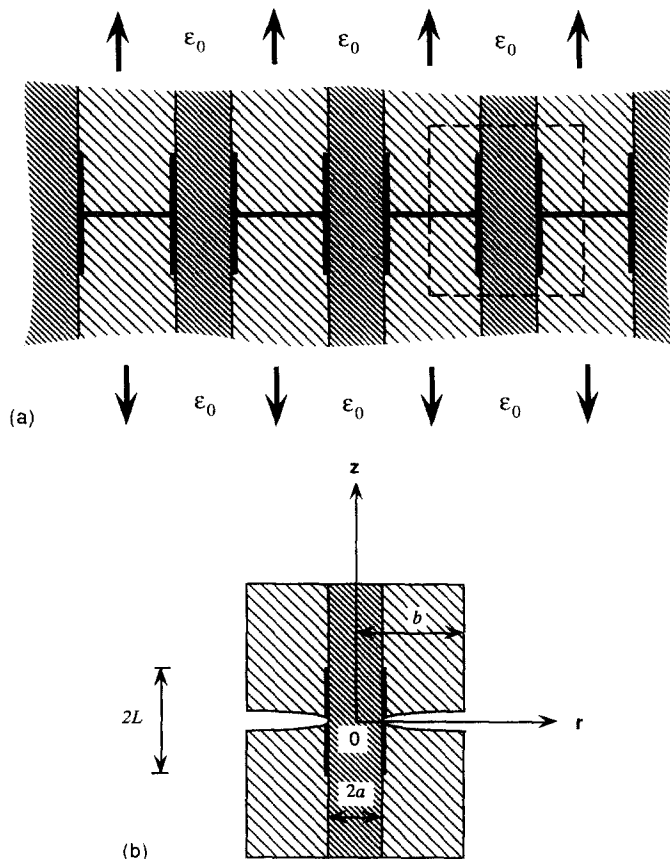
Fig. 1. Schematic of matrix cracking with interfacial slip for a fiber-reinforced brittle matrix composite undergoing longitudinal tensile loading.

The superposition procedure adopted to obtain the solution for the problem of matrix cracking with interfacial slip utilizes the following two related problems. Problem (i) consists of a crack-free uniaxially loaded composite specimen with perfect interfacial bonding and a stress-free outer boundary. Problem (ii) consists of a matrix cracked specimen shown in Fig. 1(b) loaded on the crack surface by self-equilibrating stresses which are equal and opposite to the stresses obtained from the undamaged composite in Problem (i) and which has a prescribed shear stress in the slip region. This prescribed shear stress can be regarded as a critical yield stress along the interface that cannot be exceeded. Although its value can be an arbitrary function of z, later it will be taken as constant. The problem is then analogous to a Dugdale shear crack. The outer boundary in Problem (ii) has zero radial displacement and shear stress [see e.g. Wijeyewickrema and Keer (1991)]. The complete stress fields for Problem (i) are given in their appendix.

To formulate the problem of matrix cracking with interfacial slip it is sufficient to consider only the upper half of the concentric circular cylinders model since $z = 0$ is a plane of symmetry. Love's stress functions and the associated stress fields used are given elsewhere [see Wijeyewickrema and Keer (1991)]. Here, only expressions for the matrix axial stress and fiber shear stress used to obtain the integral equations are given where the superscripts and subscripts 0 and 1 refer to the fiber and matrix respectively:

$$\sigma_{zz}^1(r,z) = \frac{2}{\pi} \int_0^\infty \{f_4(s)I_0(rs) + f_5(s)[2(2-v_1)I_0(rs) + rsI_1(rs)] + f_6(s)K_0(rs)$$

$$+ f_7(s)[-2(2-v_1)K_0(rs) + rsK_1(rs)]\}s^3 \cos(zs)\, ds$$

$$+ \int_0^\infty f_8(p)p^4(1+zp)\, e^{-zp}J_0(rp)\, dp, \quad (1)$$

$$\sigma_{rz}^0(r,z) = \frac{2}{\pi} \int_0^\infty \{f_1(s)I_1(rs) + f_2(s)[rsI_0(rs) + 2(1-v_0)I_1(rs)]\}s^3 \sin(zs)\,\mathrm{d}s$$

$$+ \int_0^\infty f_3(p)p^5 z\,\mathrm{e}^{-zp}J_1(rp)\,\mathrm{d}p, \quad (2)$$

where f_i $(i = 1, \ldots, 8)$ are functions yet to be determined, $J_n(\ )$ is the Bessel function of the first kind of order n, $I_n(\ )$ and $K_n(\ )$ are the modified Bessel functions of the first and second kind of order n and $v_i(i = 0, 1)$ the Poisson's ratio.

The conditions at the interface are given by

$$\sigma_{rr}^0(a,z) = \sigma_{rr}^1(a,z), \quad \sigma_{rz}^0(a,z) = \sigma_{rz}^1(a,z), \quad 0 \leqslant z < \infty, \quad (3)$$

$$u_r^0(a,z) = u_r^1(a,z), \quad 0 \leqslant z < \infty, \quad (4)$$

$$\sigma_{rz}^0(a,z) = \sigma_{rz}^1(a,z) = T_s\tau(z), \quad 0 \leqslant z \leqslant L, \quad (5)$$

$$u_z^0(a,z) = u_z^1(a,z), \quad L \leqslant z < \infty, \quad (6)$$

where T_s is the amplitude of the prescribed shear stress $\tau(z)$, $(|\tau(z)| \leqslant 1)$ in the slip region while the boundary conditions on the external cylindrical surface of the matrix are taken as

$$u_r^1(b,z) = 0, \quad 0 \leqslant z < \infty, \quad (7)$$

$$\sigma_{rz}^1(b,z) = 0, \quad 0 \leqslant z < \infty. \quad (8)$$

The conditions on the crack plane $z = 0$ are

$$\sigma_{rz}^0(r,0) = 0, \quad 0 \leqslant r \leqslant a; \quad \sigma_{rz}^1(r,0) = 0, \quad a \leqslant r \leqslant b, \quad (9)$$

$$\sigma_{zz}^1(r,0) = -P_c p(r), \quad a < r < b, \quad (10)$$

$$u_z^0(r,0) = 0, \quad 0 \leqslant r \leqslant a, \quad (11)$$

where P_c is the amplitude of the axial stress distribution $p(r)$, $(|p(r)| \leqslant 1)$ in the matrix of the crack-free composite due to the applied uniform longitudinal tensile strain ε_0 at $z = \pm\infty$.

Making use of the expressions for stresses and displacements given in Wijeyewickrema and Keer (1991), it can be seen that eqn (9) is identically satisfied and that from eqn (11), $f_3(p) = 0$.

An unknown function $\phi_1(r)$ which is related to the gradient of the crack opening displacement is defined in the cracked region as

$$\frac{\mu_1}{1-v_1} \frac{\partial}{\partial r} u_z^1(r,0) = \phi_1(r), \quad a < r < b \quad (12)$$

and hence it can be shown that

$$p^3 f_8(p) = \int_a^b t\phi_1(t)J_1(pt)\,\mathrm{d}t. \quad (13)$$

To account for interfacial slip a second unknown function $\phi_2(z)$ is introduced in the

slip region as follows:

$$\phi_2(z) = \mu_0 \frac{\partial}{\partial z}[u_z^1(a,z) - u_z^0(a,z)], \quad 0 < z < L. \tag{14}$$

The three continuity conditions at the interface, eqns (3) and (4), and the two boundary conditions on the external surface of the matrix, eqns (7) and (8), form the first five equations of a system of six equations for the unknown functions f_i, $(i = 1, 2, 4, 5, 6, 7)$ in terms of the unknown functions ϕ_i, $(i = 1, 2)$. The sixth equation is obtained from eqns (6) and (14). Hence the system of six eqns can be expressed as follows:

$$I_1(as)f_1(s) + asI_0(as)f_2(s) - \bar{\mu}I_1(as)f_4(s) - \bar{\mu}asI_0(as)f_5(s) + \bar{\mu}K_1(as)f_6(s) + \bar{\mu}asK_0(as)f_7(s)$$

$$= \frac{1}{s^3}\int_a^b t\phi_1(t)h_1(t,s)\,dt, \tag{15}$$

$$\left[-I_0(as) + \frac{I_1(as)}{as}\right]f_1(s) - [(1-2v_0)I_0(as) + asI_1(as)]f_2(s) + \left[I_0(as) - \frac{I_1(as)}{as}\right]f_4(s)$$

$$+ [(1-2v_1)I_0(as) + asI_1(as)]f_5(s) + \left[K_0(as) + \frac{K_1(as)}{as}\right]f_6(s)$$

$$+ [-(1-2v_1)K_0(as) + asK_1(as)]f_7(s) = \frac{1}{s^3}\int_a^b t\phi_1(t)h_2(t,s)\,dt, \tag{16}$$

$$I_1(as)f_1(s) + [asI_0(as) + 2(1-v_0)I_1(as)]f_2(s) - I_1(as)f_4(s)$$

$$- [asI_0(as) + 2(1-v_1)I_1(as)]f_5(s) + K_1(as)f_6(s)$$

$$+ [asK_0(as) - 2(1-v_1)K_1(as)]f_7(s) = \frac{1}{s^3}\int_a^b t\phi_1(t)h_3(t,s)\,dt, \tag{17}$$

$$I_1(bs)f_4(s) + bsI_0(bs)f_5(s) - K_1(bs)f_6(s) - bsK_0(bs)f_7(s) = \frac{1}{s^3}\int_a^b t\phi_1(t)h_4(t,s)\,dt, \tag{18}$$

$$I_1(bs)f_4(s) + [bsI_0(bs) + 2(1-v_1)I_1(bs)]f_5(s) - K_1(bs)f_6(s)$$

$$+ [-bsK_0(bs) + 2(1-v_1)K_1(bs)]f_7(s) = \frac{1}{s^3}\int_a^b t\phi_1(t)h_5(t,s)\,dt, \tag{19}$$

$$-\frac{1}{2}I_0(as)f_1(s) - \frac{1}{2}[4(1-v_0)I_0(as) + asI_1(as)]f_2(s) + \frac{\bar{\mu}}{2}I_0(as)f_4(s)$$

$$+ \frac{\bar{\mu}}{2}[4(1-v_1)I_0(as) + asI_1(as)]f_5(s) + \frac{\bar{\mu}}{2}K_0(as)f_6(s)$$

$$+ \frac{\bar{\mu}}{2}[-4(1-v_1)K_0(as) + asK_1(as)]f_7(s) = \frac{1}{s^3}\int_a^b t\phi_1(t)h_6(t,s)\,dt$$

$$+ \frac{1}{s^3}\int_0^L \phi_2(u)\cos(us)\,du, \tag{20}$$

where $\bar{\mu} = \mu_0/\mu_1$ and the functions h_i, $(i = 1, \ldots, 6)$ are given by

$$h_1(t,s) = \bar{\mu}s\{asI_0(as)K_1(ts) - tsI_1(as)K_0(ts) - 2(1-v_1)I_1(as)K_1(ts)\}, \tag{21}$$

$$h_2(t,s) = s\left\{tsI_0(as)K_0(ts)+I_0(as)K_1(ts)-\frac{t}{a}I_1(as)K_0(ts)-\left[as+\frac{2(1-v_1)}{as}\right]I_1(as)K_1(ts)\right\},$$

$$(22)$$

$$h_3(t,s) = s\{asI_0(as)K_1(ts)-tsI_1(as)K_0(ts)\}, \tag{23}$$

$$h_4(t,s) = s\{-tsI_0(ts)K_1(bs)+bsI_1(ts)K_0(bs)+2(1-v_1)I_1(ts)K_1(bs)\}, \tag{24}$$

$$h_5(t,s) = s\{-tsI_0(ts)K_1(bs)+bsI_1(ts)K_0(bs)\}, \tag{25}$$

$$h_6(t,s) = -\tfrac{1}{2}\bar{\mu}s\{-tsI_0(as)K_0(ts)+2(1-v_1)I_0(as)K_1(ts)+asI_1(as)K_1(ts)\}. \tag{26}$$

From the system of six equations given by eqns (15)–(20) the unknown functions f_i, ($i = 1, 2, 4, 5, 6, 7$) can be expressed in terms of ϕ_i, ($i = 1, 2$) as

$$f_i(s) = \int_a^b t\phi_1(t)\,\mathrm{d}t\frac{1}{s^3}\sum_{j=1}^{6}\frac{A_{ij}(s)h_j(t,s)}{\Delta(s)}+\int_0^L \phi_2(u)\cos(us)\,\mathrm{d}u\frac{1}{s^3}\frac{A_{i6}(s)}{\Delta(s)}, \tag{27}$$

where $\Delta(s)$ is the determinant and $A_{ij}(s)$, ($i = 1, 2, 4, 5, 6, 7; j = 1, \ldots, 6$) are the appropriate elements of the adjoint of the coefficient matrix of the system of six equations.

From eqn (10) which corresponds to the traction applied at the crack surface and eqn (5), which describes the adhesive shear stress prescribed in the slip zone and making use of eqns (1), (2), (13) and (27), the following coupled singular integral equations are obtained:

$$\frac{1}{\pi}\int_{t=a}^{b}\left\{\frac{1}{t-r}+k_{11}(r,t)\right\}\phi_1(t)\,\mathrm{d}t+\frac{1}{\pi}\int_{t=0}^{L}k_{12}(r,t)\phi_2(t)\,\mathrm{d}t = -P_c p(r), \quad a<r<b, \tag{28}$$

$$\frac{2}{\pi}\int_{t=a}^{b}t\phi_1(t)k_4(z,t)\,\mathrm{d}t+\frac{2}{\pi}\int_{t=0}^{L}\phi_2(t)k_5(z,t)\,\mathrm{d}t = T_s\tau(z), \quad 0<z<L, \tag{29}$$

where

$$k_{11}(r,t) = k_1(r,t)+2tk_2(r,t), \tag{30}$$

$$k_1(r,t) = \frac{m(r,t)-1}{t-r}+\frac{m(r,t)}{t+r}, \tag{31}$$

$$m(r,t) = \begin{cases} E(r/t), & r<t, \\ \dfrac{r}{t}E(t/r)+\dfrac{t^2-r^2}{rt}K(t/r), & r>t, \end{cases} \tag{32}$$

$$k_2(r,t) = \int_0^\infty \bar{k}_2(r,t,s)\,\mathrm{d}s, \tag{33}$$

$$\bar{k}_2(r,t,s) = \frac{1}{\Delta(s)}\left\{\left(\sum_{i=1}^{6}A_{4i}h_i\right)I_0(rs)+\left(\sum_{i=1}^{6}A_{5i}h_i\right)[2(2-v_1)I_0(rs)+rsI_1(rs)]\right.$$

$$\left.\times\left(\sum_{i=1}^{6}A_{6i}h_i\right)K_0(rs)+\left(\sum_{i=1}^{6}A_{7i}h_i\right)[-2(2-v_1)K_0(rs)+rsK_1(rs)]\right\}, \tag{34}$$

$$k_{12}(r,t) = 2k_3(r,t), \tag{35}$$

$$k_3(r, t) = \int_0^\infty \bar{k}_3(r, s) \cos (ts) \, ds, \tag{36}$$

$$\bar{k}_3(r, s) = \frac{1}{\Delta(s)} \{ A_{46} I_0(rs) + A_{56}[2(2 - v_1) I_0(rs) + rs I_1(rs)] + A_{66} K_0(rs)$$

$$+ A_{76}[-2(2 - v_1) K_0(rs) + rs K_1(rs)] \}, \tag{37}$$

$$k_4(z, t) = \int_0^\infty \bar{k}_4(t, s) \sin (zs) \, ds, \tag{38}$$

$$\bar{k}_4(t, s) = \frac{1}{\Delta(s)} \left\{ \left(\sum_{i=1}^6 A_{1i} h_i \right) I_1(as) + \left(\sum_{i=1}^6 A_{2i} h_i \right) [as I_0(as) + 2(1 - v_0) I_1(as)] \right\}, \tag{39}$$

$$k_5(z, t) = \int_0^\infty \bar{k}_5(s) \cos (ts) \sin (zs) \, ds, \tag{40}$$

$$\bar{k}_5(s) = \frac{1}{\Delta(s)} \{ A_{16} I_1(as) + A_{26}[as I_0(as) + 2(1 - v_0) I_1(as)] \}, \tag{41}$$

where $K(\ )$ and $E(\ )$ are the complete elliptic integrals of the first and second kind respectively.

SOLUTION PROCEDURE

The infinite integrals $k_2(r, t)$, $k_3(r, t)$, $k_4(z, t)$ and $k_5(z, t)$ given by eqns (33), (36), (38) and (40) can be manipulated such that eqns (28) and (29) can be rewritten as

$$\frac{1}{\pi} \int_{t_1 = a}^b \left\{ \frac{1}{t_1 - r} + l_{11s}(r, t_1) + l_{11f}(r, t_1) \right\} \phi_1(t_1) \, dt_1$$

$$+ \frac{1}{\pi} \int_{t_2 = 0}^L \{ l_{12s}(r, t_2) + l_{12f}(r, t_2) \} \phi_2(t_2) \, dt_2 = -P_c p(r), \quad a < r < b, \tag{42}$$

$$\frac{1}{\pi} \int_{t_1 = a}^b \{ l_{21s}(z, t_1) + l_{21f}(z, t_1) \} \phi_1(t_1) \, dt_1$$

$$+ \frac{2c_{51}}{\pi} \int_{t_2 = 0}^L \left\{ \frac{1}{t_2 - z} + l_{22s}(z, t_2) + l_{22f}(z, t_2) \right\} \phi_2(t_2) \, dt_2 = T_s \tau(z), \quad 0 < z < L, \tag{43}$$

where the explicit forms of the kernels are given in Appendix A. The singular behavior of ϕ_i, $(i = 1, 2)$ has been investigated by considering the dominant parts of the coupled integral equations (42) and (43) for the case where the outer crack tip is located at c ($<b$) in Appendix B. First it was shown that there is no power singularity and next that a bounded solution is not possible at the common end point ($r = a, z = 0$).

The solution of the integral equations is of the form:

$$\phi_1(t_1) = \log |t_1 - a| g_1(t_1), \quad a < t_1 < b, \tag{44}$$

$$\phi_2(t_2) = \log |t_2| (L - t_2)^{-1/2} g_2(t_2), \quad 0 < t_2 < L, \tag{45}$$

where $g_1(t_1)$ and $g_2(t_2)$ are bounded in the closed intervals $a \leqslant t_1 \leqslant b$ and $0 \leqslant t_2 \leqslant L$, respectively. From eqn (44) it is seen that $\phi_1(t_1)$ is bounded at $t_1 = b$. The limits of the

integral equations are normalized by defining:

$$t_1 = \frac{b-a}{2}\tau_1 + \frac{b+a}{2}, \quad r = \frac{b-a}{2}\rho_1 + \frac{b+a}{2}, \tag{46}$$

$$t_2 = \frac{L-0}{2}\tau_2 + \frac{L+0}{2}, \quad z = \frac{L-0}{2}\rho_2 + \frac{L+0}{2}, \tag{47}$$

$$\phi_1(t_1) = P_c(1-\tau_1)^{-1/2}(\tau_1+1)^{-1/2}F_1(\tau_1), \tag{48}$$

$$\phi_2(t_2) = P_c(1-\tau_2)^{-1/2}(\tau_2+1)^{-1/2}F_2(\tau_2), \tag{49}$$

$$L_{11s}(\rho_1,\tau_1) = \frac{b-a}{2}l_{11s}(r,t_1), \quad L_{11f}(\rho_1,\tau_1) = \frac{b-a}{2}l_{11f}(r,t_1), \tag{50}$$

$$L_{21s}(\rho_2,\tau_1) = \frac{b-a}{2}l_{21s}(z,t_1), \quad L_{21f}(\rho_2,\tau_1) = \frac{b-a}{2}l_{21f}(z,t_1), \tag{51}$$

$$L_{12s}(\rho_1,\tau_2) = \frac{L-0}{2}l_{12s}(r,t_2), \quad L_{12f}(\rho_1,\tau_2) = \frac{L-0}{2}l_{12f}(r,t_2), \tag{52}$$

$$L_{22s}(\rho_2,\tau_2) = \frac{L-0}{2}l_{22s}(z,t_2), \quad L_{22f}(\rho_2,\tau_2) = \frac{L-0}{2}l_{22f}(z,t_2), \tag{53}$$

$$p(r) = P(\rho_1), \quad \tau(z) = T(\rho_2), \tag{54}$$

to arrive at the equations:

$$\frac{1}{\pi}\int_{-1}^{+1}\left\{\frac{1}{\tau_1-\rho_1}+L_{11s}(\rho_1,\tau_1)+L_{11f}(\rho_1,\tau_1)\right\}F_1(\tau_1)(1-\tau_1)^{-1/2}(\tau_1+1)^{-1/2}\,d\tau_1$$

$$+\frac{1}{\pi}\int_{-1}^{+1}\left\{L_{12s}(\rho_1,\tau_2)+L_{12f}(\rho_1,\tau_2)\right\}F_2(\tau_2)(1-\tau_2)^{-1/2}(\tau_2+1)^{-1/2}\,d\tau_2 = -P(\rho_1),$$

$$-1 < \rho_1 < +1, \tag{55}$$

$$\frac{1}{\pi}\int_{-1}^{+1}\left\{L_{21s}(\rho_2,\tau_1)+L_{21f}(\rho_2,\tau_1)\right\}F_1(\tau_1)(1-\tau_1)^{-1/2}(\tau_1+1)^{-1/2}\,d\tau_1$$

$$+\frac{2c_{51}}{\pi}\int_{-1}^{+1}\left\{\frac{1}{\tau_2-\rho_2}+L_{22s}(\rho_2,\tau_2)+L_{22f}(\rho_2,\tau_2)\right\}$$

$$\times F_2(\tau_2)(1-\tau_2)^{-1/2}(\tau_2+1)^{-1/2}\,d\tau_2 = \frac{T_s}{P_c}T(\rho_2), -1 < \rho_2 < +1. \tag{56}$$

The coupled singular integral equations (55) and (56) are solved together with the constraint conditions (i) $F_1(+1) = 0$, which accounts for the boundedness of $\phi_1(t_1)$ at $t_1 = b$, (ii) $F_1(-1) = 0$, since $\phi_1(t_1)$ is logarithmically singular at $t_1 = a$, (iii) $F_2(-1) = 0$, since $\phi_2(t_2)$ is logarithmically singular at $t_2 = 0$ and (iv) $F_2(+1) = 0$, to account for nonsingular stresses at $z = L$.

A Gauss–Chebyshev integration formula (Erdogan et al., 1973) is used to discretize

eqns (55) and (56) to get

$$\sum_{m=1}^{M} \left\{ \frac{1}{\tau_{1,m} - \rho_{1,r}} L_{11s}(\rho_{1,r}, \tau_{1,m}) + L_{11f}(\rho_{1,r}, \tau_{1,m}) \right\} \frac{F_1(\tau_{1,m})}{M}$$

$$+ \sum_{n=1}^{N} \left\{ L_{12s}(\rho_{1,r}, \tau_{2,n}) + L_{12f}(\rho_{1,r}, \tau_{2,n}) \right\} \frac{F_2(\tau_{2,n})}{N} = -P(\rho_{1,r}), \quad r = 1, \ldots, M-1. \quad (57)$$

$$\sum_{m=1}^{M} \left\{ L_{21s}(\rho_{2,s}, \tau_{1,m}) + L_{21f}(\rho_{2,s}, \tau_{1,m}) \right\} \frac{F_1(\tau_{1,m})}{M}$$

$$+ 2c_{51} \sum_{n=1}^{N} \left\{ \frac{1}{\tau_{2,n} - \rho_{2,s}} + L_{22s}(\rho_{2,s}, \tau_{2,n}) + L_{22f}(\rho_{2,s}, \tau_{2,n}) \right\}$$

$$\times \frac{F_2(\tau_{2,n})}{N} = \frac{T_s}{P_c} T(\rho_{2,s}), \quad s = 1, \ldots, N-1, \quad (58)$$

where

$$\tau_{1,m} = \cos\left[\frac{\pi}{2M}(2m-1) \right], \quad \tau_{2,n} = \cos\left[\frac{\pi}{2N}(2n-1) \right], \quad (59)$$

$$\rho_{1,r} = \cos\left(\frac{\pi r}{M} \right), \quad\quad \rho_{2,s} = \cos\left(\frac{\pi s}{N} \right). \quad (60)$$

The additional conditions are discretized by using the formulae given by Krenk (1975). In solving the problem it was convenient to prescribe the *size* of the interfacial slip length and to *solve* for the applied load ratio T_s/P_c. The $M+N+1$ unknowns are $F_1(\tau_{1,m})$, $m = 1, \ldots, M$; $F_2(\tau_{2,n})$, $n = 1, \ldots, N$ and the ratio T_s/P_c. Since eqns (57), (58) and the four constraint conditions provide an additional equation, M is chosen to be an even number and the $M/2$ equation of equation (57) is neglected.

RESULTS AND DISCUSSION

One of the main objectives of the present study was to examine the effects of interfacial slip on a matrix crack which terminates at the interface. Hence results are first given for the normalized interfacial adhesive shear stress in the slip region for different materials and then the interfacial stresses and the matrix axial stress at different locations in a particular composite SiC/CAS. All the results are for Poisson's ratios of $v_0 = v_1 = 0.25$. As previously discussed the interfacial adhesive shear stress distribution in the slip region is assumed constant, i.e. $\tau(z) = 1.0$ in eqns (5), (29) and (43). The axial stress in the matrix σ_0, of an uncracked composite is independent of r when the outer matrix surface is stress free and is given by

$$\sigma_0 = E_1 \varepsilon_0 - 2v_1 \sigma^* \left(\frac{a^2}{b^2 - a^2} \right), \quad (61)$$

where

$$\sigma^* = \frac{2\varepsilon_0(v_0 - v_1)V_m}{V_f/k_{p1} + V_m/k_{p0} + 1/\mu_1} \quad (62)$$

and $V_f = a^2/b^2$, $V_m = 1 - V_f$ and $k_{pi} = \mu_i/(1 - 2v_i)$, $(i = 0, 1)$. (Appendix A, Wijeyewickrema

and Keer, 1991). Here μ, ν and E are the shear modulus, Poisson's ratio and Young's modulus, respectively. Hence $P_c = \sigma_0$ and $p(r) = 1.0$ in eqns (10), (28) and (42).

The SiC/CAS composite has the following material properties (Daniel *et al.*, 1989; Lee and Daniel, 1992):

$$E_0 = 207 \text{ GPa } (30.0 \times 10^6 \text{ psi}), \qquad E_1 = 98 \text{ GPa } (14.2 \times 10^6 \text{ psi}),$$

$$F_{mT} = 124 \text{ MPa } (18.0 \times \times 10^3 \text{ psi}), \quad F_{is} = 221 \text{ MPa } (32.0 \times 10^3 \text{ psi}),$$

$$\nu_0 = \nu_1 = 0.25,$$

$$V_f = 0.4, \tag{63}$$

where F_{mT} and F_{is} are the matrix tensile strength and interfacial shear strength respectively. [The value given for F_{is} is that assumed by Lee and Daniel (1992)]. The stress fields are either normalized with respect to the uncracked (far-field) matrix axial stress σ_0, i.e. $\bar{\sigma}_{zz}(a, z) = \sigma_{zz}(a, z)/\sigma_0$ etc., or by the matrix tensile strength F_{mT}, i.e. $\tilde{\sigma}_{zz}(a, z) = \sigma_{zz}(a, z)/F_{mT}$ etc. In the plots of the stress fields the stresses are compared with the case of perfect adhesion at the interface, i.e. $L = 0$.

In Figs 2(a), (b) the normalized interfacial shear stress is plotted against L/b for fiber
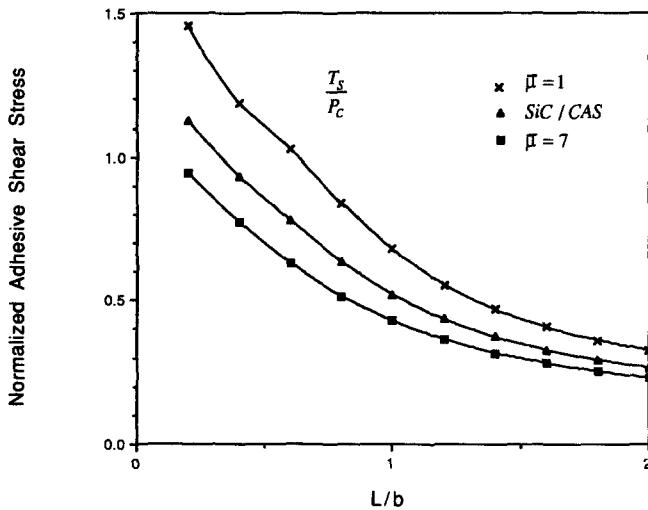
Fig. 2(a). Normalized interfacial adhesive shear stress in slip region, $V_f = 0.4$.
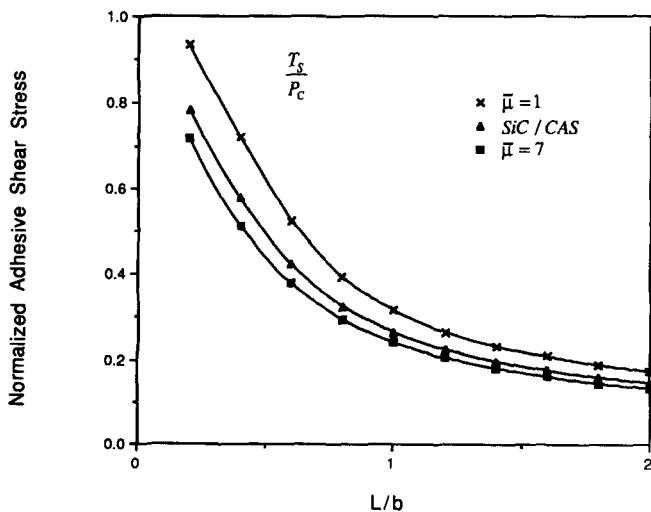

Fig. 2(b). Normalized interfacial adhesive shear stress in slip region, $V_f = 0.6$.
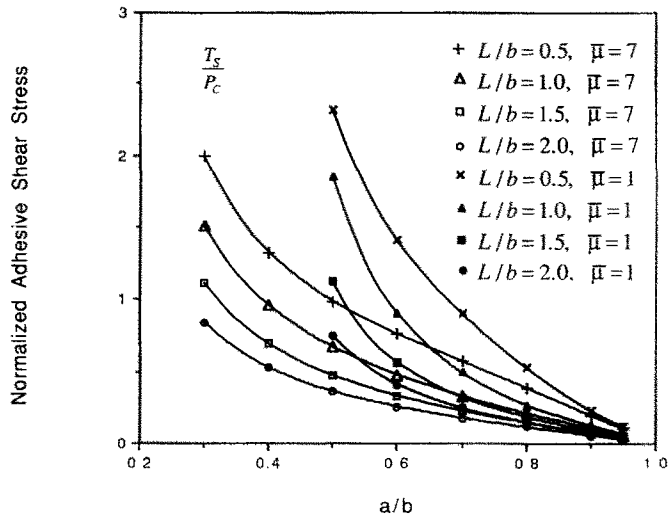
Fig. 3. Normalized interfacial adhesive shear stress in slip region for different fiber radii.
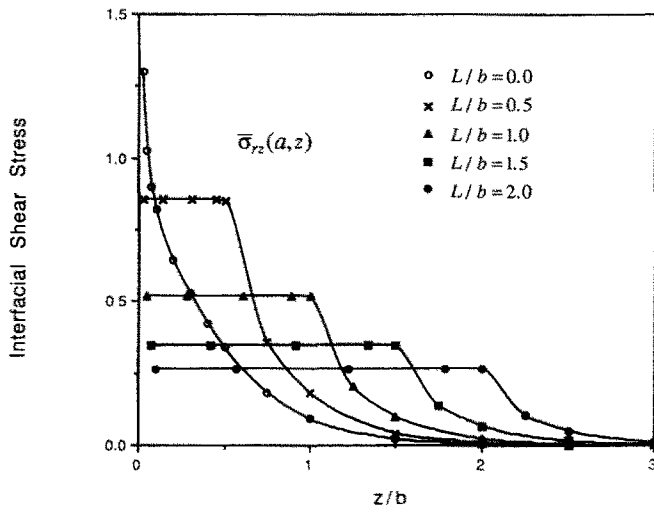

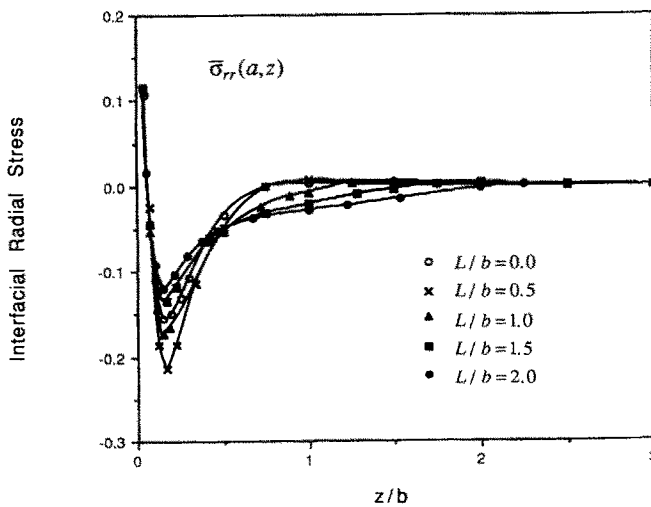Fig. 4(a). Normalized interfacial shear stress in the SiC/CAS composite for different slip lengths.

Fig. 4(b). Normalized interfacial radial stress in the SiC/CAS composite for different slip lengths.

volume ratios of $V_f = 0.4$ and 0.6, respectively. As expected, when the fiber stiffness increases for a given slip length, the interfacial shear stress decreases and this decrease is more pronounced for smaller slip lengths. It is also observed that when V_f is higher that the interfacial shear stress is lower since more load is carried by the fiber due to the increase in cross-sectional area. The effect of the fiber volume fraction on the interfacial shear stress for different slip lengths is shown in Fig. 3. A typical brittle matrix composite used in applications would have a fiber volume fraction in the range $0.3 \leqslant V_f \leqslant 0.6$ which corresponds to $0.55 \leqslant a/b \leqslant 0.77$. Figure 3 shows that for this range of a/b, the interfacial shear stress differs significantly with the slip length.

The interfacial stresses are given in Fig. 4. For the SiC/CAS composite when the slip length $L/b = 0.5$, 1.0, 1.5 and 2.0, the normalized interfacial shear stress $T_s/P_c = 0.854$, 0.519, 0.348 and 0.266, respectively. A consequence of the assumption of constant adhesive shear stress in the slip zone and hence a finite slip length is that the interfacial stresses decay
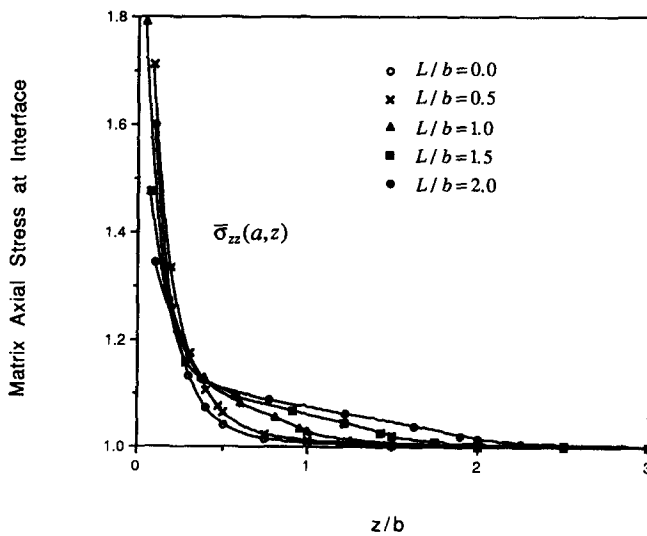
Fig. 5(a). Normalized axial stress in the matrix at the interface of the SiC/CAS composite for different slip lengths.
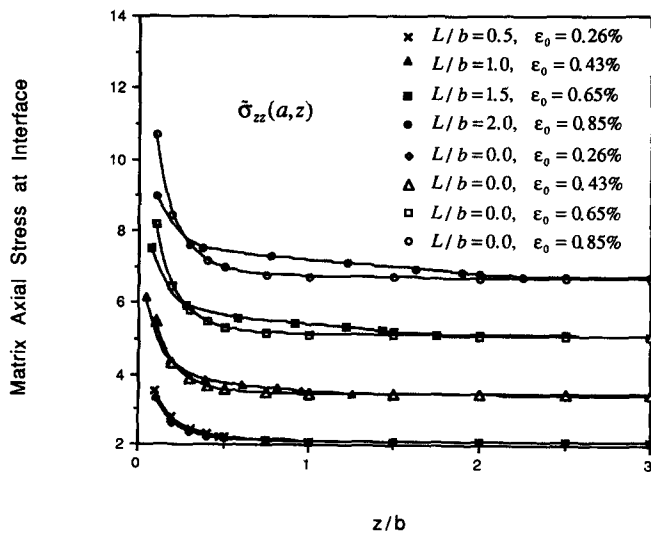
Fig. 5(b). Axial stress normalized by matrix tensile strength at the interface of the SiC/CAS composite for different slip lengths.

less rapidly away from the crack plane. Although the interfacial shear stress is finite at the crack plane $z = 0$ when there is slip, the interfacial radial stress still exhibits singular behavior. Furthermore, in the vicinity of the crack the interfacial radial stresses are tensile (Fig. 4b) which indicates that a more accurate formulation would take interfacial debonding into account there. This figure also indicates that interfacial frictional slip might occur near the debond region.

In Figs 5–8 the matrix axial stresses at different locations are plotted. In plotting Figs 5(b), 6(b) and 7(b) the interfacial shear strength F_{is} from eqn (63) has been used and when the slip length $L/b = 0.5$, 1.0, 1.5 and 2.0 the applied strain ε_0 is 0.26%, 0.43%, 0.65% and 0.85%, respectively. In Fig. 5 the axial stress in the matrix at the interface is singular at the
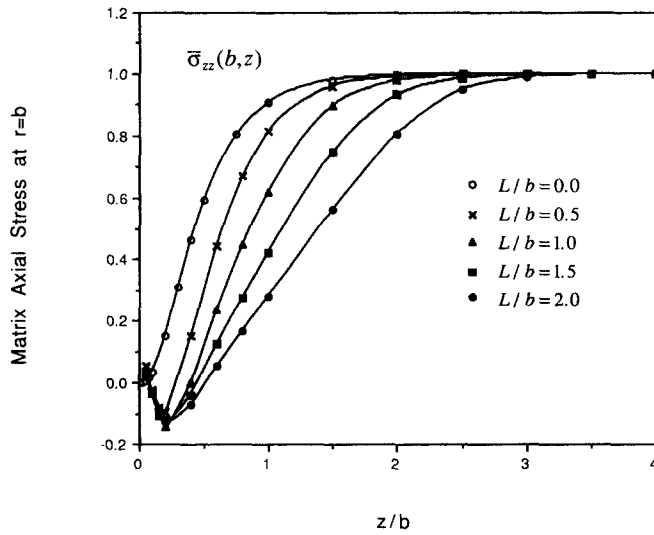

Fig. 6(a). Normalized axial stress in the matrix at $r = b$ of the SiC/CAS composite for different slip lengths.
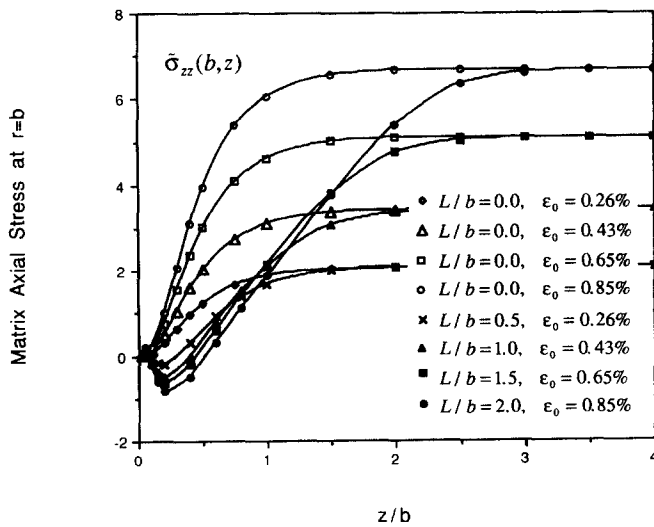

Fig. 6(b). Axial stress normalized by matrix tensile strength at $r = b$ of the SiC/CAS composite for different slip lengths.

crack plane and decreases monotonically to its far field value away from the crack plane. The matrix axial stress at $r = b$ is shown in Fig. 6. The compressive stresses close to the crack plane may be due to interfacial slip, as there are no such stresses for the fully bonded case, and here too the stresses decay less rapidly away from the crack plane when there is interfacial slip. Figure 7 shows the axial stress in the matrix in the plane located at a distance $z = b$. Since the load is transferred to the matrix through the interface, for a given slip length the matrix carries more load at the interface than at the mid-surface between fibers. If the tip of the slip zone is below the location where the stresses are computed, i.e. $z > L$ the stresses have a $1/r$ type of decay. But when the stresses are being computed along a plane intersecting the slip zone, i.e. $z < L$, then the stresses other than in a small region
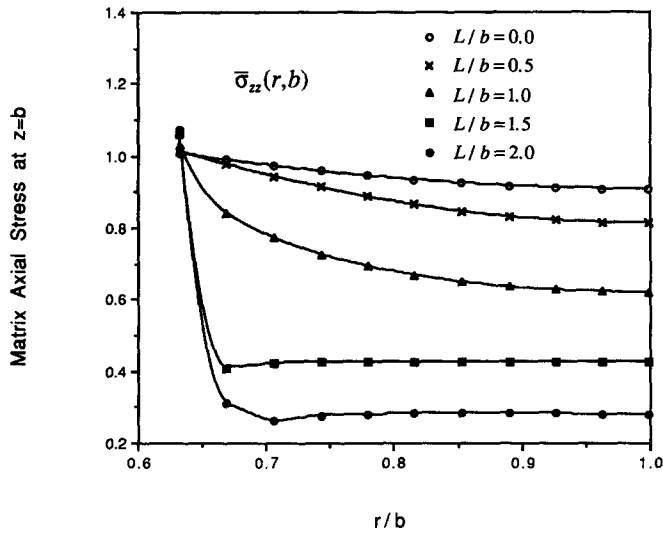

Fig. 7(a). Normalized axial stress in the matrix at $z = b$ of the SiC/CAS composite for different slip lengths.
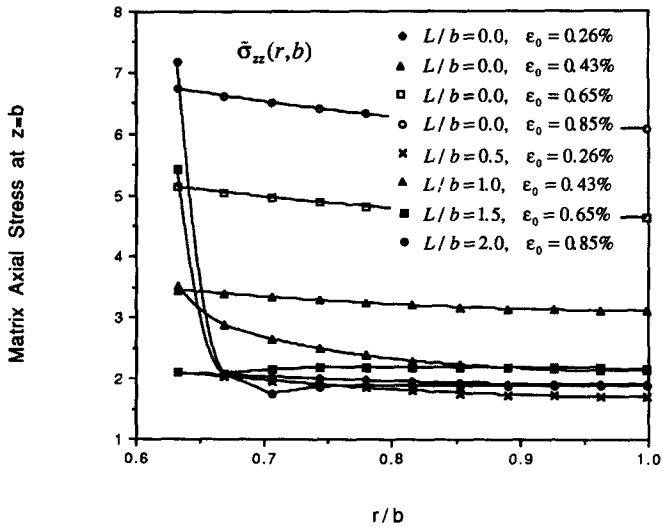

Fig. 7(b). Axial stress normalized by matrix tensile strength at $z = b$ of the SiC/CAS composite for different slip lengths.
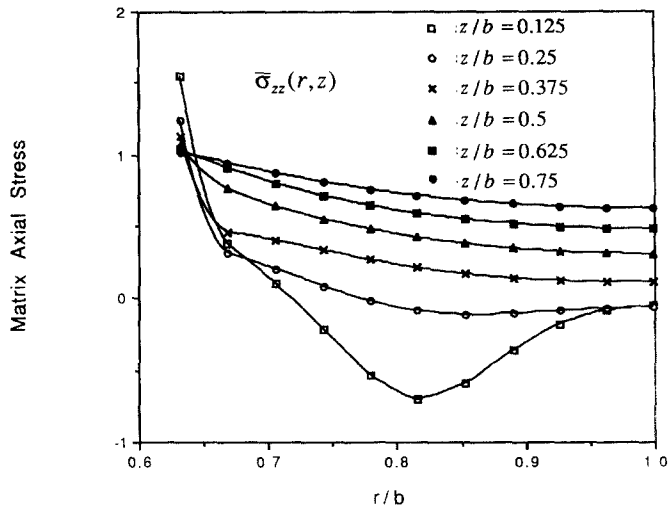
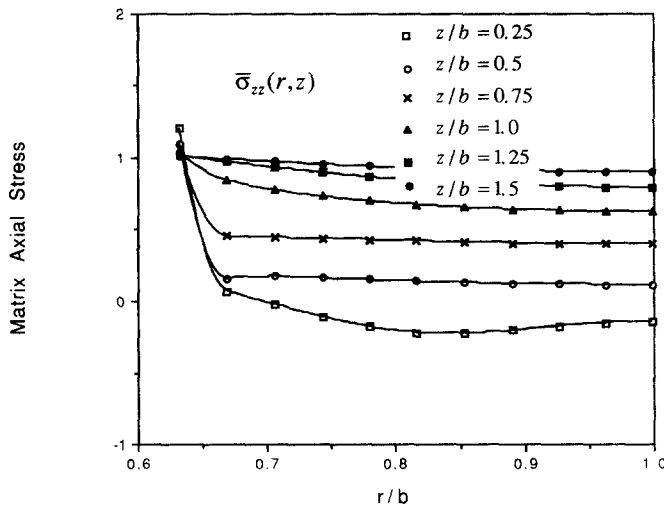Fig. 8(a). Normalized axial stress in the matrix of the SiC/CAS composite when slip length $L/b = 0.5$.

Fig. 8(b). Normalized axial stress in the matrix of the SiC/CAS composite when slip length $L/b = 1.0$.
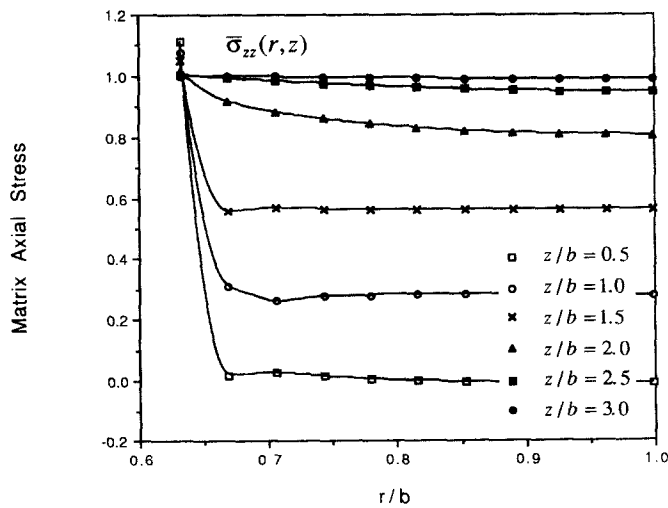

Fig. 8(c). Normalized axial stress in the matrix of the SiC/CAS composite when slip length $L/b = 2.0$.
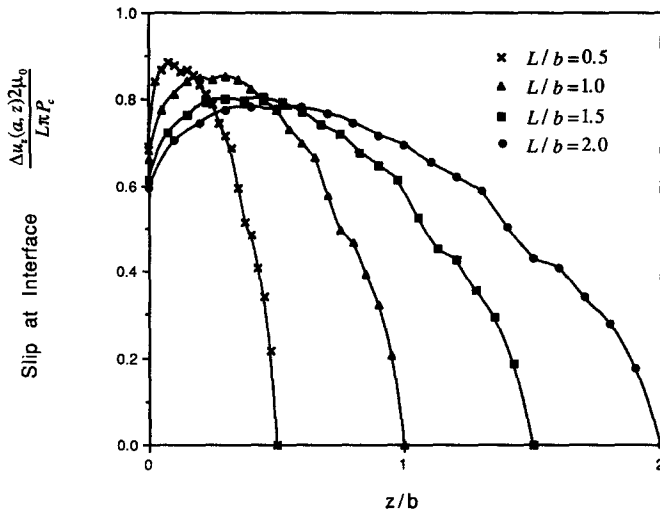
Fig. 9. Nondimensional slip at the interface of the SiC/CAS composite.

close to the interface are nearly constant. In Fig. 8 the matrix axial stress is plotted for slip lengths of $L/b = 0.5$, 1.0 and 2.0. The stress close to the crack plane is distorted due to the slip at the interface.

The interfacial slip given by $\Delta u_z(a, z) = u_z^1(a, z) - u_z^0(a, z)$, can be computed from

$$\Delta u_z(a, z) = -\frac{1}{\mu_0} \int_z^L \phi_2(t_2)\, dt_2 \tag{64}$$

and is plotted in nondimensional form in Fig. 9. Here, it is observed that the maximum slip occurs away from the crack plane and that this peak decreases with increasing slip length.

From eqn (12) the relative crack opening displacement $u_z^1(r, 0) - u_z^1(a, 0)$ is obtained as

$$u_z^1(r, 0) - u_z^1(a, 0) = \frac{1 - \nu_1}{\mu_1} \int_a^r \phi_1(t_1)\, dt_1 \tag{65}$$

and is given in Fig. 10. The absolute crack opening displacement is plotted in Fig. 11. The
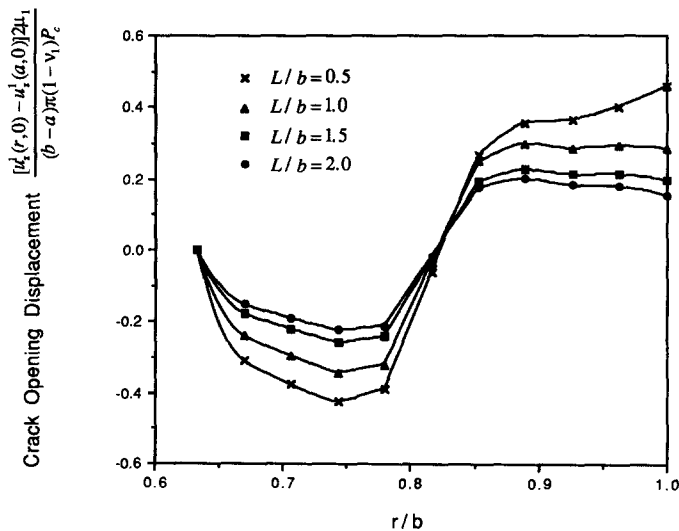

Fig. 10. Nondimensional relative crack opening displacement of the SiC/CAS composite.
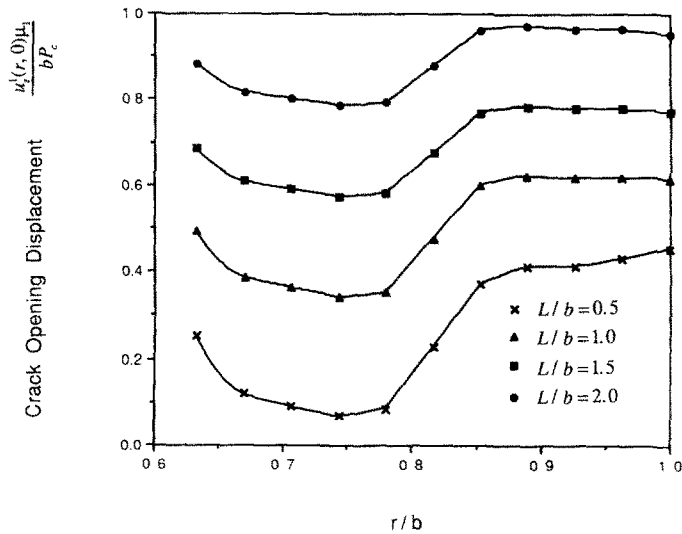
Fig. 11. Nondimensional absolute crack opening displacement of the SiC/CAS composite.

interfacial slip blunts and separates the crack tip at the interface and causes the COD to be changed from its usual opening mode. It should be noted that eqn (65) depends on points near $\phi_1(a)$. Since the singularity is not accurately taken into account there in the numerical scheme, the points close to the interface in Figs 10 and 11 may be inaccurate.

REFERENCES

Budiansky, B., Hutchinson, J. W. and Evans, A. G. (1986). Matrix fracture in fiber-reinforced ceramics. *J. Mech. Phys. Solids* 34(2), 167 189.

Daniel, I. M., Anastassopoulos, G. and Lee, J.-W. (1989). Experimental micromechanics of brittle-matrix composites. In *Micromechanics: Experimental Techniques* (Edited by W. N. Sharpe Jr.), AMD Vol. 102, pp. 133–146. ASME, New York.

Dollar, A. and Steif, P. S. (1989). A tension crack impinging upon frictional interfaces. *ASME J. Appl. Mech.* 56, 291-298.

Dundurs, J. (1969). Discussion. *ASME J. Appl. Mech.* 36, 650 652.

Erdogan, F., Gupta, G. D. and Cook, T. S. (1973). Numerical solution of singular integral equations. In *Mechanics of Fracture 1: Methods of Analysis and Solutions of Crack Problems* (Edited by G. C. Sih), pp. 368–425. Noordhoff, Leyden.

Gao, Y. C., Mai, Y.-W. and Cotterell, B. (1988). Fracture of fiber-reinforced materials. *ZAMP* 39, 550–572.

Gharpuray, V. M., Dundurs, J. and Keer, L. M. (1991). A crack terminating at a slipping interface between two materials. *ASME J. Appl. Mech.* 58, 960–963.

Hutchinson, J. W. and Jensen, H. M. (1990). Models of fiber debonding and pullout in brittle composites with friction. *Mech. Materials* 9, 139–163.

Keer, L. M. and Chen, S. H. (1981). The intersection of a pressurized crack with a joint. *J. Geophys. Res.* 86, 1032–1038.

Krenk, S. (1975). On the use of the interpolation polynomial for solutions of singular integral equations. *Q. Appl. Math.* 32, 479–484.

Lee, J.-W. and Daniel, I. M. (1992). Deformation and failure of longitudinally loaded brittle-matrix composites. In *Composite Materials: Testing and Design* (Edited by C. M. Glenn). ASTM STP 1120, pp. 204–221.

Marshall, D. B., Cox, B. N. and Evans, A. G. (1985). The mechanics of matrix cracking in brittle-matrix fiber composites. *Acta Metall.* 33(11), 2013 2021.

McCartney, L. N. (1989). New theoretical model of stress transfer between fiber and matrix in a uniaxially fibre-reinforced composite. *Proc. R. Soc. Lond., Series A,* 425, 215–244.

Sigl, L. S. and Evans, A. G. (1989). Effects of residual stress and frictional sliding on cracking and pull-out in brittle matrix composites. *Mech. Materials* 8, 1-12.

Tsai, W. B. and Mura, T. (1991). Fracture of a brittle matrix composite with strong long fibers. *Proceedings of the Sixth Technical Conference American Society for Composites,* pp. 538–547. Technomic Publishing Company, Lancaster, PA.

Wijeyewickrema, A. C. and Keer, L. M. (1991). Matrix fracture in brittle matrix fiber-reinforced composites. *Int. J. Solids Structures* 28, 43–65.

Wijeyewickrema, A. C. and Keer, L. M. (1992). Matrix crack interaction in a fiber-reinforced brittle matrix composite. *Int. J. Solids Structures* **29**, 559–570.

APPENDIX A

The kernels appearing in eqns (42) and (43) are defined in this appendix.

$$l_{11s}(r, t_1) = 2t_1 k_{2s}(r, t_1), \tag{A1}$$

$$k_{2s}(r, t) = I_{2s}^{a\infty}(r, t) + I_{2s}^{b\infty}(r, t), \tag{A2}$$

$$I_{2s}^{a\infty}(r, t) = \frac{1}{2\sqrt{rt}} \left\{ c_{21} \frac{1}{(r+t-2a)} + c_{22} \frac{(r-a)}{(r+t-2a)^2} + c_{23} \frac{(r-a)^2}{(r+t-2a)^3} \right\}, \tag{A3}$$

$$I_{2s}^{b\infty}(r, t) = \frac{1}{2\sqrt{rt}} \left(\frac{-1}{2b-r-t} \right), \tag{A4}$$

where

$$c_{21} = \frac{1}{2} \left[1 - \frac{\bar{\mu}(1+\kappa_1)}{\bar{\mu}+\kappa_0} - \frac{3(1-\bar{\mu})}{1+\bar{\mu}\kappa_1} \right], \quad c_{22} = \frac{6(1-\bar{\mu})}{1+\bar{\mu}\kappa_1}, \quad c_{23} = -\frac{4(1-\bar{\mu})}{1+\bar{\mu}\kappa_1}, \tag{A5}$$

$$l_{11f}(r, t_1) = k_1(r, t_1) + 2t_1 k_{2f}(r, t_1), \tag{A6}$$

$$k_{2f}(r, t) = \int_0^\infty [\bar{K}_2(r, t, s) - \bar{K}_2^{a\infty}(r, t, s) - \bar{K}_2^{b\infty}(r, t, s)] \, ds + I_{2f}^{a\infty}(r, t) + I_{2f}^{b\infty}(r, t), \tag{A7}$$

$$\bar{K}_2^{a\infty}(r, t, s) = (R_1^{cra}s^2 + R_2^{cra}s + R_3^{cra}) \frac{e^{-(r+t-2a)s}}{2\sqrt{rt}}, \tag{A8}$$

$$\bar{K}_2^{b\infty}(r, t, s) = (R_2^{crb}s + R_3^{crb}) \frac{e^{-(2b-r-t)s}}{2\sqrt{rt}}, \tag{A9}$$

$$I_{2f}^{a\infty}(r, t) = \frac{1}{2\sqrt{rt}} \left[\sum_{i=1}^6 S_{1i} + \sum_{i=1}^3 T_{1i} \right], \tag{A10}$$

$$I_{2f}^{b\infty}(r, t) = \frac{1}{2\sqrt{rt}} \sum_{i=1}^2 S_{2i}, \tag{A11}$$

$$l_{12s}(r, t_2) = 2k_{3s}(r, t_2), \tag{A12}$$

$$k_{3s}(r, t) = I_{3s}^{a\infty}(r, t), \tag{A13}$$

$$I_{3s}^{a\infty}(r, t) = \sqrt{\frac{a}{r}} \left\{ c_{31} \frac{(r-a)}{t^2+(r-a)^2} + c_{32} \frac{(r-a)^3}{[t^2+(r-a)^2]^2} \right\}, \tag{A14}$$

$$c_{31} = \frac{4[(4-5v_0)+\bar{\mu}(2-v_1)]}{(1+\bar{\mu}\kappa_1)(\bar{\mu}+\kappa_0)}, \quad c_{32} = -\frac{4}{1+\bar{\mu}\kappa_1}, \tag{A15}$$

$$l_{12f}(r, t_2) = 2k_{3f}(r, t_2), \tag{A16}$$

$$k_{3f}(r, t) = \int_0^\infty [\bar{K}_3(r, s) - \bar{K}_3^{a\infty}(r, s)] \cos(ts) \, ds + I_{3f}^{a\infty}(r, t), \tag{A17}$$

$$\bar{K}_3^{a\infty}(r, s) = (R_2^{sra}s + R_3^{sra}) \sqrt{\frac{a}{r}} e^{-(r-a)s}, \tag{A18}$$

$$I_{3f}^{a\infty}(r, t) = \sqrt{\frac{a}{r}} \sum_{i=1}^2 S_{3i} \tag{A19}$$

$$l_{21s}(z, t_1) = 2t_1 k_{4s}(z, t_1), \tag{A20}$$

$$k_{4s}(z, t) = I_{4s}^{a\infty}(z, t), \tag{A21}$$

$$I_{4s}^{a\infty}(z, t) = \frac{1}{2\sqrt{at}} \left\{ c_{41} \frac{z}{(t-a)^2+z^2} + c_{42} \frac{z^3}{[(t-a)^2+z^2]^2} \right\}, \tag{A22}$$

$$c_{41} = \frac{8\bar{\mu}(1-v_1)(-2+3v_0-\bar{\mu}v_1)}{(1+\bar{\mu}\kappa_1)(\bar{\mu}+\kappa_0)}, \quad c_{42} = \frac{8\bar{\mu}(1-v_1)}{(1+\bar{\mu}\kappa_1)}, \quad (A23)$$

$$l_{21f}(z, t_1) = 2t_1 k_{4f}(z, t_1), \quad (A24)$$

$$k_{4f}(z, t) = \int_0^\infty [\bar{k}_4(t, s) - \bar{k}_4^{a\infty}(t, s)] \sin(zs)\, \mathrm{d}s + I_{4f}^{a\infty}(z, t), \quad (A25)$$

$$\bar{k}_4^{a\infty}(t, s) = (R_2^{cr0}s + R_3^{cr0})\frac{e^{-(t-a)s}}{2\sqrt{at}}, \quad (A26)$$

$$I_{4f}^{a\infty}(z, t) = \frac{1}{2\sqrt{at}}\sum_{i=1}^2 S_{4i}, \quad (A27)$$

$$l_{22s}(z, t_2) = -\frac{1}{t_2 + z}, \quad (A28)$$

$$l_{22f}(z, t_2) = \frac{1}{c_{51}}k_{5f}(z, t_2), \quad (A29)$$

$$c_{51} = \frac{2[\bar{\mu}(1-v_1)+(1-v_0)]}{(1+\bar{\mu}\kappa_1)(\bar{\mu}+\kappa_0)}, \quad (A30)$$

$$k_{5f}(z, t) = \int_0^\infty [\bar{k}_5(s) - \bar{k}_5^\infty(s)] \cos(ts)\sin(zs)\, \mathrm{d}s + I_{5f}^\infty(z, t), \quad (A31)$$

$$\bar{k}_5^\infty(s) = R_3^{sr0} + R_4^{sr0}\frac{1}{s}, \quad (A32)$$

$$I_{5f}^\infty(z, t) = R_4^{sr0}\frac{\pi}{2}H(z-t), \quad (A33)$$

and $\kappa_i = 3-4v_i$; $(i = 0, 1)$ and $H(\ )$ is the Heaviside step function.

The functions R_i^{cra}, $(i = 1-3)$; R_i^{crb}, $(i = 2, 3)$; R_i^{sra}, $(i = 2, 3)$; R_i^{cr0}, $(i = 2, 3)$ and R_i^{sr0}, $(i = 3, 4)$ appearing in eqns (A8), (A9), (A18), (A26) and (A32) are given by

$$R_1^{cra} = \frac{P_1^{cra}}{Q_1}, \quad R_2^{cra} = \frac{1}{Q_1}\left(P_2^{cra} - P_1^{cra}\frac{Q_2}{Q_1}\right), \quad R_3^{cra} = \frac{1}{Q_1}\left[P_3^{cra} - P_2^{cra}\frac{Q_2}{Q_1} + P_1^{cra}\left(-\frac{Q_3}{Q_1} + \frac{Q_2^2}{Q_1^2}\right)\right], \quad (A34)$$

$$R_2^{crb} = \frac{P_2^{crb}}{Q_1}, \quad R_3^{crb} = \frac{1}{Q_1}\left(P_3^{crb} - P_2^{crb}\frac{Q_2}{Q_1}\right), \quad (A35)$$

$$R_2^{sra} = \frac{P_2^{sra}}{Q_1}, \quad R_3^{sra} = \frac{1}{Q_1}\left(P_3^{sra} - P_2^{sra}\frac{Q_2}{Q_1}\right), \quad (A36)$$

$$R_2^{cr0} = \frac{P_2^{cr0}}{Q_1}, \quad R_3^{cr0} = \frac{1}{Q_1}\left(P_3^{cr0} - P_2^{cr0}\frac{Q_2}{Q_1}\right), \quad (A37)$$

$$R_3^{sr0} = \frac{P_3^{sr0}}{Q_1}, \quad R_4^{sr0} = \frac{1}{Q_1}\left(P_4^{sr0} - P_3^{sr0}\frac{Q_2}{Q_1}\right), \quad (A38)$$

where

$$P_1^{cra} = 2(1-v_1)(1-\bar{\mu})(\bar{\mu}+\kappa_0)(r-a)(t-a), \quad (A39)$$

$$P_2^{cra} = (1-v_1)(1-\bar{\mu})\{2(\bar{\mu}+\kappa_0)(r-a) - 3(\bar{\mu}+\kappa_0)(r+t-2a) + p_{21}^{cra}[(r-a)(r+t-2a) - (r-a)^2]\}, \quad (A40)$$

$$P_3^{cra} = (1-v_1)\{(1-\bar{\mu})p_{31}^{cra}(r-a) + (1-\bar{\mu})p_{32}^{cra}(r+t-2a) + (1-\bar{\mu})p_{33}^{cra}[(r-a)(r+t-2a)$$
$$-(r-a)^2] + 2[\kappa_0 - 2\bar{\mu}v_1(1-2v_0) + \bar{\mu}^2(-3+6v_1-4v_1^2)]\}, \quad (A41)$$

$$P_2^{crb} = (1-v_1)(\bar{\mu}+\kappa_0)(1+\bar{\mu}\kappa_1)(2b-r-t), \quad (A42)$$

$$P_3^{crb} = (1-v_1)[p_{31}^{crb}(2b-r-t) - 2(\bar{\mu}+\kappa_0)(1+\bar{\mu}\kappa_1)], \quad (A43)$$

$$P_2^{sra} = -2(1-v_1)(\bar{\mu}+\kappa_0)(r-a), \quad (A44)$$

$$P_3^{sra} = (1-v_1)\{p_{31}^{sra}(r-a) + 2[(5-6v_0) + \bar{\mu}(3-2v_1)]\}, \quad (A45)$$

$$P_2^{cr0} = -4\bar{\mu}(1-\nu_1)^2(\bar{\mu}+\kappa_0)(t-a), \tag{A46}$$

$$P_3^{cr0} = (1-\nu_1)^2\bar{\mu}\{p_{31}^{cr0}(t-a)+8[\bar{\mu}(1-\nu_1)+(1-\nu_0)]\}, \tag{A47}$$

$$P_3^{tr0} = -4(1-\nu_1)[\bar{\mu}(1-\nu_1)+(1-\nu_0)], \tag{A48}$$

$$P_4^{tr0} = (1-\nu_1)\left\{\frac{4}{a}[\bar{\mu}(1-\nu_1)(1-2\nu_0)-(1-\nu_0)(1-2\nu_1)]+\frac{3}{b}[\bar{\mu}(1-\nu_1)+(1-\nu_0)]\right\}, \tag{A49}$$

$$p_{21}^{cra} = (\bar{\mu}+\kappa_0)\left(-\frac{3}{2b}+\frac{3}{4t}-\frac{1}{4r}\right)-\frac{1}{2a}[(5+7\bar{\mu})-4\nu_0(1+2\bar{\mu})], \tag{A50}$$

$$p_{31}^{cra} = \frac{3}{16t}[(29+15\bar{\mu})-4\nu_0(9+2\bar{\mu})]+\left(\frac{1}{16r}-\frac{3}{4a}\right)[(5+7\bar{\mu})-4\nu_0(1+2\bar{\mu})]-\frac{3}{2b}(\bar{\mu}+\kappa_0), \tag{A51}$$

$$p_{32}^{cra} = \frac{9}{8}\left(\frac{2}{b}-\frac{1}{t}\right)(\bar{\mu}+\kappa_0)+\frac{1}{16r}[(1-5\bar{\mu})+4\nu_0(-1+2\bar{\mu})]+\frac{1}{16a}[(-19+63\bar{\mu})+4\nu_0(15-26\bar{\mu})+32\nu_1(\bar{\mu}+\kappa_0)], \tag{A52}$$

$$p_{33}^{cra} = \frac{3}{16a^2}[(-7+19\bar{\mu})+4\nu_0(1-4\bar{\mu})]+\frac{3}{8ab}[(5+7\bar{\mu})-4\nu_0(1+2\bar{\mu})]$$

$$+\frac{3}{16}\left(-\frac{1}{b^2}+\frac{1}{br}+\frac{3}{4r^2}-\frac{5}{4t^2}-\frac{3}{bt}-\frac{1}{2rt}\right)(\bar{\mu}+\kappa_0), \tag{A53}$$

$$p_{31}^{crb} = -\frac{1}{2a}(1-\bar{\mu}^2)(1-\kappa_0\kappa_1)+\frac{1}{8}\left(\frac{1}{r}-\frac{3}{t}\right)(\bar{\mu}+\kappa_0)(1+\bar{\mu}\kappa_1), \tag{A54}$$

$$p_{31}^{sra} = \frac{1}{4r}(\bar{\mu}+\kappa_0)+\frac{3}{2b}(\bar{\mu}+\kappa_0)+\frac{1}{4a}[(1+11\bar{\mu})+4\nu_0(1-4\bar{\mu})], \tag{A55}$$

$$p_{31}^{cr0} = -\frac{3}{2t}(\bar{\mu}+\kappa_0)+\frac{3}{b}(\bar{\mu}+\kappa_0)+\frac{1}{2a}[(1+11\bar{\mu})+4\nu_0(1-4\bar{\mu})], \tag{A56}$$

$$Q_1 = (1-\nu_1)(\bar{\mu}+\kappa_0)(1+\bar{\mu}\kappa_1), \tag{A57}$$

$$Q_2 = -\frac{1}{2}(1-\nu_1)\left[\frac{1}{a}(1-\bar{\mu}^2)(1-\kappa_0\kappa_1)+\frac{3}{2b}(\bar{\mu}+\kappa_0)(1+\bar{\mu}\kappa_1)\right], \tag{A58}$$

$$Q_3 = \frac{1}{32}(1-\nu_1)\left\{-\frac{8}{a^2}(1-\bar{\mu})\{\bar{\mu}[(1+\kappa_0\kappa_1)+4(\nu_0-2\nu_1)]-[(1+\kappa_0\kappa_1)+4(\nu_1-2\nu_0)]\}\right.$$

$$\left.+\frac{12}{ab}(1-\bar{\mu}^2)(1-\kappa_0\kappa_1)-\frac{3}{b^2}(\bar{\mu}+\kappa_0)(1+\bar{\mu}\kappa_1)\right\}. \tag{A59}$$

The functions S_{1i}, $(i = 1,\ldots,6)$ and T_{1i}, $(i = 1-3)$ required to define $I_{2f}^{a\infty}(r, t)$ in eqn (A10) are expressed as

$$S_{11} = -\frac{P_1^{cra}Q_2}{Q_1^2}\frac{1}{(r+t-2a)^2}, \tag{A60}$$

$$S_{12} = \frac{(1-\bar{\mu})p_{21}^{cra}}{(\bar{\mu}+\kappa_0)(1+\bar{\mu}\kappa_1)}\frac{(r-a)}{(r+t-2a)}, \tag{A61}$$

$$S_{13} = \frac{-(1-\bar{\mu})p_{21}^{cra}}{(\bar{\mu}+\kappa_0)(1+\bar{\mu}\kappa_1)}\frac{(r-a)^2}{(r+t-2a)^2}, \tag{A62}$$

$$S_{14} = -\frac{P_2^{cra}Q_2}{Q_1^2}\frac{1}{(r+t-2a)}, \tag{A63}$$

$$S_{15} = \frac{(1-\bar{\mu})p_{31}^{cra}}{(\bar{\mu}+\kappa_0)(1+\bar{\mu}\kappa_1)}\frac{(r-a)}{(r+t-2a)}, \tag{A64}$$

$$S_{16} = \frac{(1-\bar{\mu})p_{32}^{cra}}{(\bar{\mu}+\kappa_0)(1+\bar{\mu}\kappa_1)}, \tag{A65}$$

$$T_{11} = \frac{P_1^{cra}}{Q_1}\left(-\frac{Q_3}{Q_1}+\frac{Q_2^2}{Q_1^2}\right)\frac{1}{(r+t-2a)}, \tag{A66}$$

$$T_{12} = \frac{(1-\bar{\mu})p_{33}^{cra}}{(\bar{\mu}+\kappa_0)(1+\bar{\mu}\kappa_1)}(r-a),$$

(A67)

$$T_{13} = -\frac{(1-\bar{\mu})p_{33}^{cra}}{(\bar{\mu}+\kappa_0)(1+\bar{\mu}\kappa_1)}\frac{(r-a)^2}{(r+t-2a)}.$$

(A68)

The functions S_{2i}, $(i = 1, 2)$ required to define $I_{2f}^{h\gamma}(r, t)$ in eqn (A11) are given by

$$S_{21} = -\frac{P_2^{crb}Q_2}{Q_1^2}\frac{1}{(2b-r-t)},$$

(A69)

$$S_{22} = \frac{p_{31}^{crb}}{(\bar{\mu}+\kappa_0)(1+\bar{\mu}\kappa_1)}.$$

(A70)

The functions S_{3i}, $(i = 1, 2)$ required to define $I_{3f}^{a\gamma}(r, t)$ in eqn (A19) are given by

$$S_{31} = -\frac{P_2^{cra}Q_2}{Q_1^2}\frac{(r-a)}{t^2+(r-a)^2},$$

(A71)

$$S_{32} = \frac{p_{31}^{cra}}{(\bar{\mu}+\kappa_0)(1+\bar{\mu}\kappa_1)}\frac{(r-a)^2}{t^2+(r-a)^2}.$$

(A72)

The functions S_{4i}, $(i = 1, 2)$ required to define $I_{4f}^{a\gamma}(z, t)$ in eqn (A27) are given by

$$S_{41} = -\frac{P_2^{cr0}Q_2}{Q_1^2}\frac{z}{(t-a)^2+z^2}.$$

(A73)

$$S_{42} = \frac{(1-\nu_1)\bar{\mu}p_{31}^{cr0}}{(\bar{\mu}+\kappa_0)(1+\bar{\mu}\kappa_1)}\frac{(t-a)z}{(t-a)^2+z^2}.$$

(A74)

APPENDIX B

In this appendix the singular nature of ϕ_i, $(i = 1, 2)$ is analysed by investigating the dominant parts of the coupled integral equations (42) and (43). Here the more general case where the matrix is not fully cracked, i.e. the outer matrix crack tip is at a point c ($<b$), is considered. The dominant parts of eqns (42) and (43) are

$$\frac{1}{\pi}\int_{t=a}^{c}\left\{\frac{1}{t-r}+2tk_{2ss}(r,t)\right\}\phi_1(t)\,dt+\frac{1}{\pi}\int_{t=0}^{L}2k_{3ss}(r,t)\phi_2(t)\,dt = R_1(r), \quad a < r < c,$$

(B1)

$$\frac{1}{\pi}\int_{t=a}^{c}\sqrt{\frac{t}{a}}\phi_1(t)\left\{e_1\frac{z}{(t-a)^2+z^2}+e_2\frac{z^3}{[(t-a)^2+z^2]^2}\right\}\,dt+\frac{1}{\pi}\int_{t=0}^{l}\left\{\frac{1}{t-z}-\frac{1}{t+z}\right\}\phi_2(t)\,dt = R_2(z), \quad 0 < z < L.$$

(B2)

where

$$k_{2ss}(r,t) = \frac{1}{2\sqrt{rt}}\left\{c_2(r-a)^2\frac{d^2}{dr^2}(r+t-2a)^{-1}+c_1(r-a)\frac{d}{dr}(r+t-2a)^{-1}+c_0(r+t-2a)^{-1}\right\},$$

(B3)

$$k_{3ss}(r,t) = \sqrt{\frac{a}{r}}\left\{d_1\frac{(r-a)^3}{[t^2+(r-a)^2]^2}+d_2\frac{(r-a)}{t^2+(r-a)^2}\right\},$$

(B4)

$$e_1 = \frac{2\bar{\mu}(1-\nu_1)[-2+3\nu_0-\bar{\mu}\nu_1]}{[\bar{\mu}(1-\nu_1)+(1-\nu_0)]}, \quad e_2 = \frac{2\bar{\mu}(\bar{\mu}+\kappa_0)(1-\nu_1)}{[\bar{\mu}(1-\nu_1)+(1-\nu_0)]},$$

(B5)

and $c_0 = c_{21}$, $c_1 = -c_{22}$, $c_2 = 2c_{23}$, $d_1 = c_{32}$, $d_2 = c_{31}$; $R_1(r)$ and $R_2(z)$ consists of the parts of the integral equations with bounded kernels.

The unknown functions ϕ_i, $(i = 1, 2)$ are expressed as

$$\phi_1(t) = f(t)(c-t)^{\alpha_0}(t-a)^{\beta_0} = f(t)\,e^{-\pi i\alpha_0}(t-c)^{\alpha_0}(t-a)^{\beta_0}, \quad a < t < c,$$

(B6)

$$\phi_2(t) = g(t)(L-t)^{\gamma_0}(t-0)^{\beta_0} = g(t)\,e^{-\pi i\gamma_0}(t-L)^{\gamma_0}(t-0)^{\beta_0}, \quad 0 < t < L.$$

(B7)

where $f(t)$ is Hölder-continuous in $a < t < c$, $(t-c)^{\alpha_0}(t-a)^{\beta_0}$ is a definite branch which varies continuously in $a < t < c$, $f(a) \neq 0$, $f(c) \neq 0$, $-1 < \text{Re}(\alpha_0, \beta_0) < 0$ and where $g(t)$ is Hölder-continuous in $0 < t < L$, $(t-L)^{\gamma_0}(t-0)^{\beta_0}$ is a definite branch varying continuously in $0 < t < L$ and $g(0) \neq 0$, $g(L) \neq 0$, $-1 < \text{Re}(\gamma_0, \beta_0) < 0$. Note that ϕ_i, $(i = 1, 2)$ must have the same singular behavior at the common end point as indicated by the index β_0.

The sectionally holomorphic functions are introduced as

$$F(z_1) = \frac{1}{\pi} \int_a^c \frac{\phi_1(t)}{t-z_1} \, dt, \quad G(z_2) = \frac{1}{\pi} \int_0^L \frac{\phi_2(t)}{t-z_2} \, dt. \tag{B8}$$

Examining the singular behavior of $F(z_1)$ and $G(z_2)$ near the end points yields

$$F(z_1) = -f(a)(c-a)^{\alpha_0} \frac{e^{-\pi i \beta_0}}{\sin \pi \beta_0}(z_1-a)^{\beta_0} + f(c)(c-a)^{\beta_0} \frac{1}{\sin \pi \alpha_0}(z_1-c)^{\alpha_0} + F_0(z_1) \tag{B9}$$

$$\frac{1}{\pi} \int_a^c \frac{\phi_1(t)}{t-r} \, dt = F(r) = -f(a)(c-a)^{\alpha_0} \cot \pi \beta_0 (r-a)^{\beta_0} + f(c)(c-a)^{\beta_0} \cot \pi \alpha_0 (c-r)^{\alpha_0} + F_1(r), \tag{B10}$$

$$\frac{1}{\pi} \int_a^c \frac{\phi_1(t)}{t-(2a-r)} \, dt = F(2a-r) = -\frac{f(a)(c-a)^{\alpha_0}(r-a)^{\beta_0}}{\sin \pi \beta_0} + F_2(r), \tag{B11}$$

$$\frac{1}{\pi}(r-a)^k \int_a^c \phi_1(t) \frac{d^k}{dr^k}(r+t-2a)^{-1} \, dt = -\frac{f(a)(c-a)^{\alpha_0}}{\sin \pi \beta_0} \beta_0(\beta_0-1)(\beta_0-2) \ldots (\beta_0-k+1)(r-a)^{\beta_0}$$
$$+ (r-a)^k \frac{d^k}{dr^k} F_2(r), \quad (k=1,2), \tag{B12}$$

$$\frac{1}{\pi} \int_a^c \frac{z}{(t-a)^2+z^2} \phi_1(t) \, dt = \frac{f(a)(c-a)^{\alpha_0}(z-0)^{\beta_0} \sin \frac{\pi \beta_0}{2}}{\sin \pi \beta_0} + F_3(z), \tag{B13}$$

$$\frac{1}{\pi} \int_a^c \frac{z^3}{[(t-a)^2+z^2]^2} \phi_1(t) \, dt = \frac{f(a)(c-a)^{\alpha_0}(z-0)^{\beta_0}(1-\beta_0) \sin \frac{\pi \beta_0}{2}}{2 \sin \pi \beta_0} + F_4(z), \tag{B14}$$

$$G(z_2) = -g(0)(L-0)^{\gamma_0} \frac{e^{-\pi i \beta_0}}{\sin \pi \beta_0}(z_2-0)^{\beta_0} + g(L)(L-0)^{\beta_0} \frac{1}{\sin \pi \gamma_0}(z_2-L)^{\gamma_0} + G_0(z_2), \tag{B15}$$

$$\frac{1}{\pi} \int_0^L \frac{\phi_2(t)}{t-z} \, dt = G(z) = -g(0)(L-0)^{\gamma_0} \cot \pi \beta_0 (z-0)^{\beta_0} + g(L)(L-0)^{\beta_0} \cot \pi \gamma_0 (L-z)^{\gamma_0} + G_1(z), \tag{B16}$$

$$\frac{1}{\pi} \int_0^L \frac{\phi_2(t)}{t+z} \, dt = G(-z) = -\frac{g(0)(L-0)^{\gamma_0}(z-0)^{\beta_0}}{\sin \pi \beta_0} + G_2(z), \tag{B17}$$

$$\frac{1}{\pi} \int_0^L \frac{(r-a)}{t^2+(r-a)^2} \phi_2(t) \, dt = \frac{g(0)(L-0)^{\gamma_0}(r-a)^{\beta_0} \sin \frac{\pi \beta_0}{2}}{\sin \pi \beta_0} + G_3(r), \tag{B18}$$

$$\frac{1}{\pi} \int_0^L \frac{(r-a)^3}{[t^2+(r-a)^2]^2} \phi_2(t) \, dt = \frac{g(0)(L-0)^{\gamma_0}(r-a)^{\beta_0}(1-\beta_0) \sin \frac{\pi \beta_0}{2}}{2 \sin \pi \beta_0} + G_4(r), \tag{B19}$$

where the functions F_i, $(i=0,\ldots,4)$ and G_i, $(i=0,\ldots,4)$ are bounded or have weaker singularities at the ends.
Now substituting from eqns (B10), (B11), (B12), (B18) and (B19) into eqn (B1) and multiplying the resulting equation first by $(c-r)^{-\alpha_0}$ and letting $r \to c$ and next by $(r-a)^{-\beta_0}$ and letting $r \to a$ the following equations are obtained:

$$f(c)(c-a)^{\beta_0} \cot \pi \alpha_0 = 0, \tag{B20}$$

$$\frac{-f(a)(c-a)^{\alpha_0}}{\sin \pi \beta_0}\{\cos \pi \beta_0 + c_2 \beta_0(\beta_0-1) + c_1 \beta_0 + c_0\} + \frac{g(0)(L-0)^{\gamma_0} 2 \sin \frac{\pi \beta_0}{2}\{\frac{1}{2}(1-\beta_0)d_1 + d_2\}}{\sin \pi \beta_0} = 0. \tag{B21}$$

Similarly substituting from eqns (B13), (B14), (B16) and (B17) into eqn (B2), and multiplying the resulting equation first by $(L-z)^{-\gamma_0}$ and letting $z \to L$ and next by $(z-0)^{-\beta_0}$ and letting $z \to 0$ the following equations are obtained:

$$g(L)(L-0)^{\beta_0} \cot \pi \gamma_0 = 0, \tag{B22}$$

$$\frac{f(a)(c-a)^{\alpha_0} \sin \frac{\pi \beta_0}{2}}{\sin \pi \beta_0}\{e_1 + \frac{1}{2}(1-\beta_0)e_2\} + \frac{g(0)(L-0)^{\gamma_0}}{\sin \pi \beta_0}[1-\cos \pi \beta_0] = 0. \tag{B23}$$

From eqns (B20) and (B22) the values of α_0 and γ_0 satisfying the condition $-1 < \mathrm{Re}\,(\alpha_0, \gamma_0) < 0$ are $\alpha_0 = -1/2$ and $\gamma_0 = -1/2$ respectively. The case of $\alpha_0 = -1/2$ corresponds to the square root singularity for a crack tip embedded in a homogeneous, isotropic elastic medium. The case $\gamma_0 = -1/2$ corresponds to the square root singularity for the tip of a crack lying in an interface which is not permitted to open in mode I but is allowed to slip in mode II. The characteristic eqn required to determine β_0 is obtained from eqns (B21) and (B23) and is given by

$$\cos \pi\beta_0 - (1-\alpha)\beta_0^2 - 2(1-\alpha)\beta_0 + \alpha = 0, \tag{B24}$$

where

$$\alpha = \frac{\bar{\mu}(1-v_1) - (1-v_0)}{\bar{\mu}(1-v_1) + (1-v_0)}, \tag{B25}$$

is the Dundurs constant (Dundurs, 1969). Equation (B24) is the same characteristic equation obtained by Gharpuray *et al.* (1991) when the planar problem of an edge crack terminating at a slipping interface was considered. For the range $-1 < \mathrm{Re}\,(\beta_0) < 0$, eqn (B24) has no roots and hence ϕ_i, $(i = 1, 2)$ has no power singularity at the common end point $(r = a, z = 0)$.

Next the possibility of a logarithmic singularity at $r = a, z = 0$ is investigated by looking for a solution of the form

$$\phi_1(t) = f_0(t)(c-t)^{\alpha_0} = f_0(t)\,\mathrm{e}^{-\pi i \alpha_0}(t-c)^{\alpha_0}, \quad a < t < c, \tag{B26}$$

$$\phi_2(t) = g_0(t)(L-t)^{\gamma_0} = g_0(t)\,\mathrm{e}^{-\pi i \gamma_0}(t-L)^{\gamma_0}, \quad 0 < t < L, \tag{B27}$$

where $f_0(a), f_0(c), g_0(0)$ and $g_0(L)$ are bounded and nonzero. Examining the singular behavior of $F(z_1)$ and $G(z_2)$ introduced previously in eqn (B8) near the end points the following asymptotic relations are obtained:

$$F(z_1) = -\frac{1}{\pi} f_0(a)(c-a)^{\alpha_0} \log (z_1 - a) + \frac{f_0(c)}{\sin \pi\alpha_0}(z_1 - c)^{\alpha_0} + C_0(z_1), \tag{B28}$$

$$\frac{1}{\pi} \int_a^c \frac{\phi_1(t)}{t-r}\,\mathrm{d}t = F(r) = -\frac{1}{\pi} f_0(a)(c-a)^{\alpha_0} \log (r-a) + f_0(c) \cot \pi\alpha_0(c-r)^{\alpha_0} + C_1(r), \tag{B29}$$

$$\frac{1}{\pi} \int_a^c \frac{\phi_1(t)}{t-(2a-r)}\,\mathrm{d}t = F(2a-r) = -\frac{1}{\pi} f_0(a)(c-a)^{\alpha_0} \log [-(r-a)] + C_2(r), \tag{B30}$$

$$\frac{1}{\pi}(r-a) \int_a^c \phi_1(t)\frac{\mathrm{d}}{\mathrm{d}r}(r+t-2a)^{-1}\,\mathrm{d}t = C_3(r), \tag{B31}$$

$$\frac{1}{\pi}(r-a)^2 \int_a^c \phi_1(t)\frac{\mathrm{d}^2}{\mathrm{d}r^2}(r+t-2a)^{-1}\,\mathrm{d}t = C_4(r), \tag{B32}$$

$$\frac{1}{\pi} \int_a^c \frac{z}{(t-a)^2 + z^2}\,\phi_1(t)\,\mathrm{d}t = C_5(z), \tag{B33}$$

$$\frac{1}{\pi} \int_a^c \frac{z^3}{[(t-a)^2 + z^2]^2}\,\phi_1(t)\,\mathrm{d}t = C_6(z), \tag{B34}$$

$$G(z_2) = -\frac{1}{\pi} g_0(0)(L-0)^{\gamma_0} \log (z_2 - 0) + \frac{g_0(L)}{\sin \pi\gamma_0}(z_2 - L)^{\gamma_0} + C_7(z_2), \tag{B35}$$

$$\frac{1}{\pi} \int_0^L \frac{\phi_2(t)}{t-z}\,\mathrm{d}t = G(z) = -\frac{1}{\pi} g_0(0)(L-0)^{\gamma_0} \log (z-0) + g_0(L) \cot \pi\gamma_0(L-z)^{\gamma_0} + C_8(z). \tag{B36}$$

$$\frac{1}{\pi} \int_0^L \frac{\phi_2(t)}{t+z}\,\mathrm{d}t = G(-z) = -\frac{1}{\pi} g_0(0)(L-0)^{\gamma_0} \log [(z-0)\,\mathrm{e}^{i\pi}] + C_9(z), \tag{B37}$$

$$\frac{1}{\pi} \int_0^L \frac{(r-a)}{t^2 + (r-a)^2}\,\phi_2(t)\,\mathrm{d}t = C_{10}(r), \tag{B38}$$

$$\frac{1}{\pi} \int_0^L \frac{(r-a)^3}{[t^2 + (r-a)^2]^2}\,\phi_2(t)\,\mathrm{d}t = C_{11}(r), \tag{B39}$$

where the functions C_i, $(i = 0, 1, \ldots, 11)$ are bounded.

Substituting from eqns (B29)–(B32), (B38) and (B39) into eqn (B1) and multiplying this equation first by

$(c-r)^{-\alpha_0}$ and letting $r \to c$ and next by $1/\log (r-a)$ and letting $r \to a$ the equations obtained are

$$f_0(c) \cot \pi\alpha_0 = 0, \tag{B40}$$

$$f_0(a)(c-a)^{\alpha_0}(1+c_0) = 0. \tag{B41}$$

Similarly substituting from eqns (B33), (B34), (B36) and (B37) into eqn (B2) it can be shown that

$$g_0(L) \cot \pi\gamma_0 = 0. \tag{B42}$$

Since eqn (B41) cannot be satisfied, a solution which is bounded at $r = a$, $z = 0$ is not possible.